Fluorescence properties of trivalent europium doped in various niobate codoped glasses

Jiwei Wang, Hongwei Song, Xianggui Kong, Hongshang Peng, Baojuan Sun et al.

Related Articles

Mechanism of the enhancement of mid-infrared emission from GeS2-Ga2S3 chalcogenide glass-ceramics doped with Tm3+
Appl. Phys. Lett. 100, 231910 (2012)

Phase evolution and room-temperature photoluminescence in amorphous SiC alloy
J. Appl. Phys. 111, 103526 (2012)

Silicon nanocluster sensitization of erbium ions under low-energy optical excitation
J. Appl. Phys. 111, 094314 (2012)

Energy transfer and energy level decay processes in Tm3+-doped tellurite glass
J. Appl. Phys. 111, 063105 (2012)

Green and red emission for (K0.5Na0.5)NbO3:Pr ceramics
J. Appl. Phys. 111, 046102 (2012)
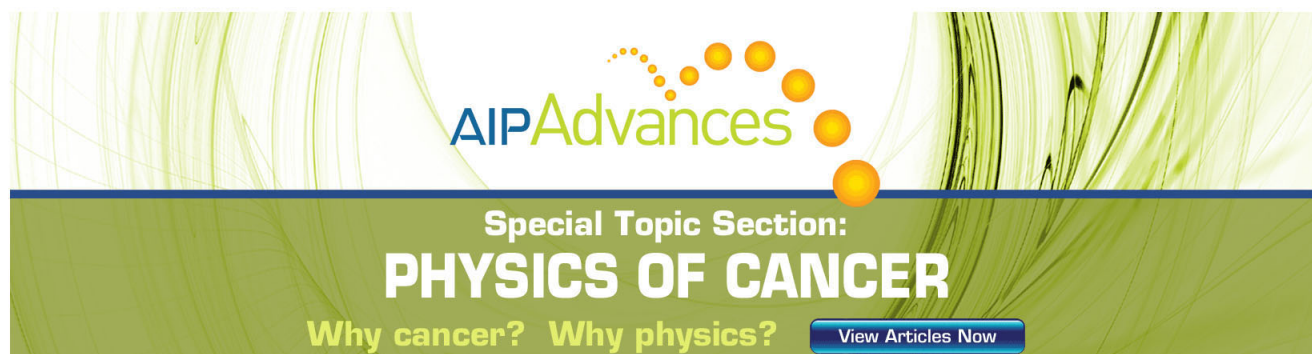
Additional information on J. Appl. Phys.

Journal Homepage: http://jap.aip.org/
Journal Information: http://jap.aip.org/about/about_the_journal
Top downloads: http://jap.aip.org/features/most_downloaded
Information for Authors: http://jap.aip.org/authors

Fluorescence properties of trivalent europium doped in various niobate codoped glasses

Jiwei Wang, Hongwei Song,[a] Xianggui Kong, Hongshang Peng, Baojuan Sun, Baojiu Chen, Jiahua Zhang, and Wu Xu
Key Laboratory of Excited State Physics, Changchun Institute of Optics, Fine Mechanics and Physics, Chinese Academy of Sciences, Changchun 130022, People's Republic of China

Haiping Xia
Laboratory of Photoelectric Materials, Ningbo University, Ningbo 315211, People's Republic of China

A series of niobate–phosphate and niobate–silicate glasses doped with Eu^{3+} ions were prepared. The emissions, phonon-side band spectra, and fluorescence lifetimes of these glasses were studied and the intensity parameters of Eu^{3+} were obtained. The temperature dependence of emission intensity of the Eu^{3+} ion in these niobate glasses was investigated. The temperature-quenching rates were determined. The results indicate that in niobate glasses, as the concentration of Nb_2O_5 increases, the covalence becomes stronger, the symmetry becomes lower and the electron-phonon coupling strength becomes stronger. Thus, the lifetimes become shorter, and the nonradiative transition processes and the temperature-quenching effect become stronger. © *2003 American Institute of Physics.* [DOI: 10.1063/1.1536726]

I. INTRODUCTION

Glasses containing rare earth ions have attracted much attention as potential materials for various optical devices such as lasers, up-conversation, stimulated phosphor, and high-density optical storage.[1,2] Among these glasses, the Eu^{3+}-doped ones are attracting great interest. Persistent spectral hole burning can be performed in the $^7F_0-^5D_0$ transition of Eu^{3+} at room temperature. This has potential use in high-density optical storage.[3–5] Compared to crystals, glasses have proven favorable as hosts for high-density memory devices due to their broad inhomogeneous width. Oxide glasses, in particular, have proven favorable as host materials for rare earth elements because of their high transparency, compositional variety, and because they are easy to mass-produce. Actually, the Eu^{3+} ion is also an activator to study local structure as well as crystal field effect.[6–8] Knowledge of local structure surrounding rare-earth ions in glasses is important not only for interpreting their optical properties. It is also useful for designing laser glasses or phosphors.[9,10] Nb_2O_5 as well as P_2O_5, SiO_2, B_2O_3, and TeO_2 has more viscosity and can form the network of glass, however, it is seldom used as a common adjuvant. Recently, we prepared niobate–phosphate and niobate–silicate glasses and studied the temperature-dependent luminescent properties of Eu^{3+} in various niobate glasses. We hoped to learn the relationship between the fluorescent properties and the local structure surrounding rare earth ions.

II. EXPERIMENTS

A. Sample preparation

Two kinds of niobate glass containing normally 1.0 wt % of Eu_2O_3 were prepared by melting. The composition of the these glasses were $Nb_2O_5-SiO_2-BaO-Na_2O$ and $Nb_2O_5-P_2O_5-BaO-Na_2O$, respectively. These glasses were named Nb–Si and Nb–P. Their detailed chemical compositions were listed in Table I. During the preparation, all of the original materials (commercial available) were mixed together and stirred until the mixture became homogeneous, then put into a kiln with an oxygenating atmosphere. After being kept at 1450 °C for 4 h and allowed to slowly cool to room temperature, these brown transparent lumps of glass were formed. These were cut into 1 cm×1 cm pieces, which were thoroughly polished.

TABLE I. Compositions of the host glasses.

Niobium phosphae glasses	P_2O_5	Nb_2O_5	BaO	Na_2O
Nb–P1	50	5	45	
Nb–P2	45	10	25	20
Nb–P3	45	15	20	20
Niobium silicate glasses	SiO_2	Nb_2O_5	BaO	Na_2O
Nb–Si1	50	5	20	25
Nb–Si2	45	10	20	25
Nb–Si3	45	15	15	25
Nb–Si4	45	20	10	25

[a]Author to whom correspondence should be addressed; electronic mail: songhongwei2000@sina.com.cn

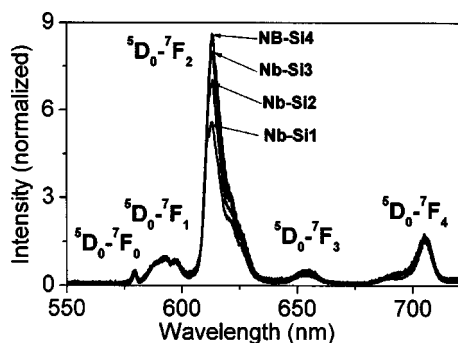J. Appl. Phys., Vol. 93, No. 3, 1 February 2003

Wang *et al.*   1483

FIG. 1. Emission spectra of the Eu^{3+} ion in niobate–silicate glasses. The emission intensities of $^5D_0-^7F_1$ are normalized in all samples.

B. Measurements

The excitation spectra of Eu^{3+} were measured with a Hitachi F-4500 fluorescence spectrophotometer, monitoring the $^5D_0-^7F_2$ transition at 612 nm. By means of the excitation spectra, the phonon sideband associated with the $^7F_0-^5D_2$ zero phonon transition was detected in the wavelength range of 430–465 nm. While measuring fluorescence lifetimes, a 266 nm light generated from the fourth-harmonic generator was combined with a Nd yttrium–aluminum–garnet pulsed laser (with a pulse width of 10 ns and a repetition frequency of 10 Hz) used as pumping. A Boxcar averager and a Spex 1403 spectrometer were used in detection.

While measuring temperature-dependent emissions of Eu^{3+}, the samples were put into a liquid nitrogen cycling system, in which the temperature varied from 77 to 691 K. A continuous 488 nm beam from an argon laser was used as excitation. The fluorescence was measured with a UV-Lab Raman Infinity (made by Jobin Yvon Company) with a resolution of 2 cm^{-1}.

III. RESULTS AND DISCUSSIONS

A. Glasses composition and its influence on luminescent properties

Figure 1 shows the emission spectra of the Eu^{3+} ions in the niobate–silicate glasses. Emissions of $^5D_0-^7F_J$ ($J=0, 1, 2, 3, 4$) transitions can be observed in all the glasses. The relative intensity of $^5D_0-^7F_2/^5D_0-^7F_1$ in the niobate–silicate glasses obviously increases as the composition of Nb_2O_5 increases. Actually, the relative intensity of $^5D_0-^7F_2/^5D_0-^7F_1$ has only a small variation with composition in the niobate–phosphate glasses. The $^5D_0-^7F_2$ transition is electric-dipole allowed and its intensity is sensitive to the local structure surrounding the Eu^{3+} ions. On the other hand, the $^5D_0-^7F_1$ transition is magnetic-dipole allowed and its intensity shows very little variation with the crystal field strength acting on the Eu^{3+} ion. Therefore, the intensity ratio of the electric-dipole to magnetic-dipole transition is widely used for the study of the chemical bond of anions coordinating the rare earth ions. The variation of the intensity ratio of $^5D_0-^7F_2/^5D_0-^7F_1$ as well as that of $^5D_0-^7F_4/^5D_0-^7F_1$ with glass composition is listed in Table II. It is obvious that the intensity ratio increases as the concentration of Nb_2O_5

increases and that of BaO decreases, indicating that the Eu–O bonds become stronger and the covalency of Eu–O bond increases.[3,11]

The intensity ratio of the electric-dipole to the magnetic-dipole transition can be written as[12–14]

$$\frac{\int I_J(\sigma)d\sigma}{\int I_{md}(\sigma)d\sigma} = \frac{e^2\sigma_J^3(n^2+2)}{9n^2 S_{nd}\sigma_{md}^3}\Omega_t \times \langle \Psi J \| U^t \| \Psi' J'\rangle^2, \quad (1)$$

where S_{md} is magnetic dipole operator, Ω_t is the intensity parameters, U^t is the reduced matrix elements, n is the refraction of the glasses, σ is the wave number of the transitions, and e is the electron mass. S_{md} is a constant which can be calculated from hybrid wave function,[15,16] Ω_t is characteristic of each ion-matrix combination, and U^t is not sensitive to the host.

Based on Eq. (1), the fluorescence intensity ratio of $^5D_0-^7F_2/D_0-^7F_1$ and the ratio of $^5D_0-^7F_4/^5D_0-^7F_1$, the values of Ω_2 and Ω_4 were obtained, as shown in Table II. Actually, Ω_2 presents ligand symmetry and the structure order. The larger the value of Ω_2, the stronger the covalence and the lower the symmetry. The values of Ω_2 in the silicate glasses are larger than that of phosphate glasses and increase with the concentration of Nb_2O_5, indicating the covalence becomes stronger and the symmetry becomes lower.

We also measured the fluorescence decay curves for the $^5D_0-^7F_2$ transition of Eu^{3+} ions at room temperature. The exponential lifetimes of $^5D_0$ in various niobate glasses were listed in Table II. It is obvious that the lifetime of $^5D_0$ becomes short with the increasing of Nb_2O_5 in both niobate–phosphate and niobate–silicate glasses. The lifetime of $^5D_0$ in niobate–silicate glasses is shorter than that in the niobate–phosphate glasses and changes more rapidly with glass composition. This means that as the system becomes disorder, the lifetime becomes short.

B. Phonon sidebands and electron-phonon coupling

Phonon sideband spectrum is a useful technique to investigate the local structure surrounding rare-earth ions in the glass network. Figures 2(a) and 2(b) show the phonon sideband spectra of Eu^{3+}, in niobate–phosphate and niobate–silicate glasses, respectively. A weak band varying from 500 to 800 cm^{-1} was observed in both the two glass series. This band is assigned to be Nb–O bonds in the NbO_6 octahedra. In the niobate–phosphate glasses, a strong band varying between 850 and 1300 cm^{-1} was observed. It was

TABLE II. Variation of intensity ratio of $^5D_0-^7F_2/^5D_0-^7F_1$ and $^5D_0-^7F_4/^5D_0-^7F_1$ and intensity parameters Ω_2, Ω_4, and lifetime of $^5D_0$.

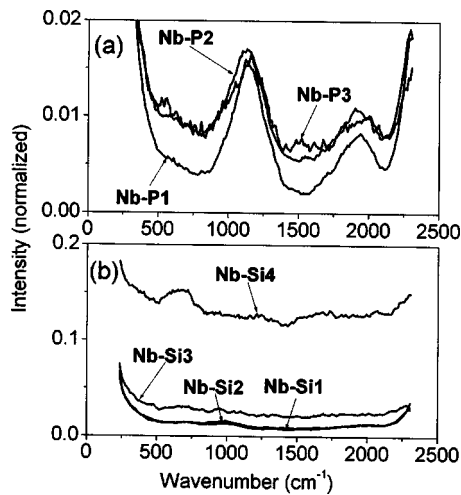| Biobate glasses	I_2/I_1	I_4/I_1	Ω_2 (10^{-20} cm^2)	Ω_4 (10^{-20} cm^2)	Lifetime (μs)
Nb–P1	4.08	1.55	7.30	5.76	2084
Nb–P2	4.22	1.55	7.55	5.76	1952
Nb–P3	4.25	1.43	7.61	5.32	1913
Nb–Si1	5.82	1.60	10.2	6.00	1463
Nb–Si2	6.99	2.11	12.3	7.91	1197
Nb–Si3	8.10	1.68	14.3	6.30	1023
Nb–Si4	8.86	1.62	15.6	6.08	867

FIG. 2. Phonon sideband spectra of Eu^{3+} in various niobate glasses, (a) niobate–phosphate glasses and (b) niobate–silicate glasses. The excitation intensities of $^7F_0-^5D_2$ are normalized in all the glasses.

FIG. 4. Normalized emission intensity of $\Sigma_J\,^5D_0-^7F_J$ as a function of temperature. The dots are experimental data and the solid lines are fitting functions, (a) niobate–silicate glasses and (b) niobate–phosphate glasses.

assigned to the symmetric stretching of PO_4 at 970 cm^{-1}, $P-O^-$ stretching mode at 1060 cm^{-1}, P–O bridge bond of PO_3 at 1140 cm^{-1}, O–P–O bond symmetric stretching at 1205 cm^{-1}, and asymmetric stretching at 1250 cm^{-1}, and P=O stretching between 1080 and 1350 cm^{-1}. In these vibrational modes, the $P-O^-$ stretching mode at 1060 cm^{-1}, the P–O bridge bond of PO_3 at 1140 cm^{-1}, and the O–P–O bond symmetric stretching at 1205 cm^{-1} were strong.[18–21] A band from 1600 to 2100 cm^{-1} was observed in the niobate–phosphate as well as the niobate–silicate glasses. It was stronger in niobate–phosphate glasses. This band is not related to any vibrational mode of the glass compositions. It is attributed to the OH groups, such as HO–P–OH and $(Si-O)_3\equiv Si-OH$.[17] In the niobate–silicate glasses, the bands from 800 to 1300 cm^{-1} were observed, which assigned to be various stretching modes of Si–O–Si.[18–21] It should be noted that in Raman spectra, the Ba–O vibrational modes appear in the range of 180–350 cm^{-1} in the two series of glasses. In the phonon sideband spectra, the Ba–O modes are emerged by the zero phonon lines of $^7F_0-^5D_2$.

It should be noted that the intensities of the zero phonon line of $^7F_0-^5D_2$ were normalized in all the glasses. Thus, the electron-phonon coupling strength can be evaluated from the integrated intensity of the phonon sideband.[8] It is clear
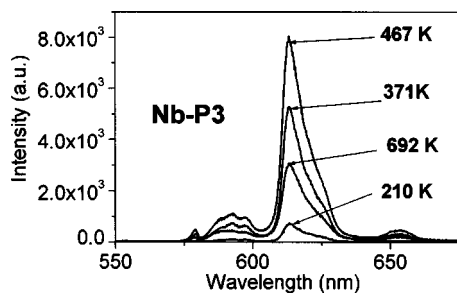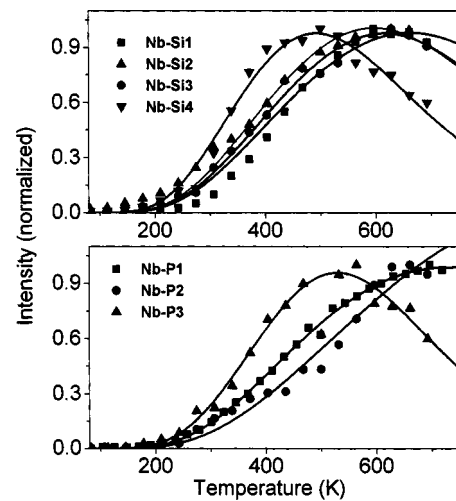
that the electron-phonon coupling becomes stronger as the concentration of N_2O_5 increases in the two series.

C. Dependence of the emission intensity of Eu^{3+} on temperature

Figure 3 shows the emission spectra of the Eu^{3+} ions at various temperatures in Nb–P3. It is obvious that the emission intensity of the Eu^{3+} ion increases with temperature and approaches a maximum at a certain temperature, then decreases as temperature increases continuously. Also, we also measured the temperature dependence of the emissions of the Eu^{3+} ion in the other glasses. Figure 4 shows the temperature dependence of the emission intensity of the Eu^{3+} ion in all the glasses. It is obvious that a maximum emission intensity appears at a certain temperature for all the glasses. The temperature of the maximum emission intensity varies, depending on the glass composition. The higher the concentration of Nb_2O_5, the lower the temperature at the maximum emission intensity.

The variation in the emission intensity of Eu^{3+} can be attributed to two main factors, the resonant $^7F_2-^5D_2$ transi-
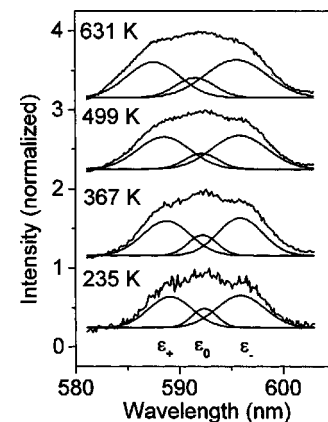

FIG. 3. Emission spectra of the Eu^{3+} ion in the Nb–P3 sample at various temperatures.

FIG. 5. Resolved emission spectra of the three crystal-field-splitting lines of the $^5D_0-^7F_1$ transition at various temperatures in the Nb–P1 glass.

TABLE III. A list of parameters β_1, β_2, and T_c (K) in various glasses.

Niobate glasses	β_1	β_2	T_c (K)
Nb–P1	34	0.0066	175
Nb–P2	56	0.0053	128
Nb–P3	57	0.0024	98
Nb–Si1	40	0.0083	159
Nb–Si2	53	0.0114	146
Nb–Si3	45	0.0056	135
Nb–Si4	97	0.0022	127

FIG. 7. Dependence of peak location of (a) $^5D_0-^7F_1$ and (b) $^5D_0-^7F_0$ transition of Eu^{3+} in the Nb–P1 on temperature.

tion with the 488 nm light and the temperature-quenching effect. The former tends to cause the intensity of Eu^{3+} to increase with temperature, while the later tends to cause the intensity to decrease.[22] The temperature-quenching channels include the nonradiative transitions from $^5D_0$ to each ^7F_J level and the energy transfer from one excited Eu^{3+} ion to the other Eu^{3+} ions or to the other centers nearby. As the contribution of the temperature-quenching effect is dominant in comparison with that of the thermal population of $^7F_2$, the emission intensity of the Eu^{3+} ion should decrease. Theoretically, the emission intensity of Σ_J $^5D_0-^7F_J$, $I(T)$, can be written approximately as
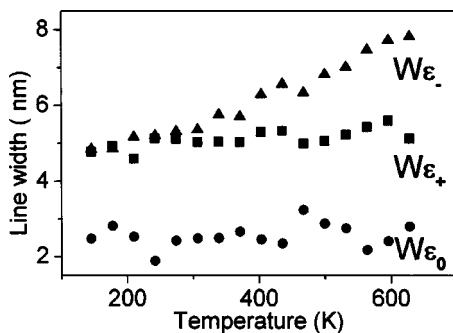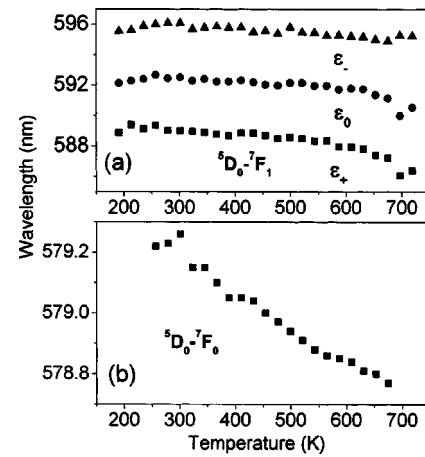
$$I(T) \propto \frac{\Phi N_2(T)\sigma}{1+W_T(T)/\gamma_0}, \qquad (2)$$

where Φ is the power density of the pumping light, W_T is the temperature-quenching rate, γ_0 is the radiative transition rate of Σ_J $^5D_0-^7F_J$, N_2 is the electron population on $^7F_2$, σ is the absorption cross section from $^7F_2$ to $^5D_2$. The normalized thermal population on ^7F_J, can be expressed as

$$N_J(T) = \frac{g_J e^{-\Delta E_J/kT}}{\Sigma_J g_J e^{-\Delta E_J/kT}}, \qquad (3)$$

where ΔE_J is the energy separation from ^7F_J to $^7F_0$, k is Boltzmann's constant, and g_J is number of Stark splitting of ^7F_J. The temperature-quenching rate is experimentally determined as[22]

$$W_T = W_T(0)e^{T/T_C}. \qquad (4)$$

FIG. 6. Dependence of linewidth of $^5D_0-^7F_1$ transition in the Nb–P1 glass on temperature.

$W_T(0)$ is the temperature-quenching rate at 0 K, T_c is a temperature constant. Based on Eqs. (2)–(4), the emission intensity of the Eu^{3+} ion as a function of temperature can be rewritten as

$$I(T) \approx \frac{\beta_1 e^{-E_2/kT}}{(1+3e^{-E_1/kT}+5e^{-E_2/kT})\times(1+\beta_2 e^{T/T_C})}, \qquad (5)$$

where $\beta_1 = 5\Phi\sigma_2$, $\beta_2 = W_T(0)/\gamma_0$.

Using Eq. (5), we well fitted the experimental data. The fitting functions were shown in Fig. 4. By fitting, the parameters β_1, β_2, T_C were determined, as shown in Table III. The nonradiative relaxation and nonradiative energy transfer processes are phonon-assisted ones and related with local structure surrounding Eu^{3+} ions. It is observed that the temperature-quenching rate increases with the increasing concentration of Nb_2O_5 and the decreasing concentration of BaO in both the niobate–phosphate and niobate–silicate glasses. This can be explained from the fact that the electron-phonon coupling becomes strong as the concentration of Nb_2O_5 increases, which is confirmed by the phonon side-band spectra.

D. Dependence of the peak location and linewidth on temperature

Figure 5 shows the lines of $^5D_0-^7F_1$ at various temperatures. The $^5D_0-^7F_1$ transition should have three Stark splitting peaks. As shown in Fig. 5, the lines of $^5D_0-^7F_1$ transition can be resolved into three Guassian components (ϵ_-, ϵ_0, and ϵ_+). Figure 6 shows the linewidths of these components as a function of temperature. It is obvious that the width of ϵ_- broadens remarkable as the temperature increases, while that of the other two components have a little variation. Figures 7(a) and 7(b) show the temperature dependence of the locations of the three Stark components of $^5D_0-^7F_1$ and of the peak location of $^5D_0-^7F_0$, respectively. It is apparent that the peak locations all shift to high-energy side as the temperature increases. We suggest that under the excitation of the 488 nm light, the electrons are resonantly excited to $^5D_2$ and then relax to $^5D_0$ through $^5D_1$. Actually, the $^5D_0$ level has a certain width in the glasses. The thermal

distribution rate of electrons in $^5D_0$ is much faster than the radiative transition rate of $^5D_0 - {}^7F_J$. As the temperature increases, more electrons populate on the top of the level based on Boltzmann distribution, and the radiative transition line of $^5D_0 - {}^5F_J$ blueshifts.

IV. CONCLUSION

In this article, we studied the spectroscopic properties of niobate–phosphate and niobate–silicate glasses doped with Eu^{3+} ions. The intensity parameter Ω_2 increases with the increasing concentration of Nb_2O_5, indicating that the symmetry has become lower. As the concentration of Nb_2O_5 increases, the electron-phonon coupling becomes stronger, and the lifetime of $^5D_0$ becomes shorter.

The temperature-dependent behavior of the Eu^{3+} ion was studied in various niobate glasses. The variation of the emission intensity of Eu^{3+} with temperature was attributed to two factors, the thermally excited emission from $^7F_2$ to $^5D_2$ and the temperature-quenching effect. The former tends to cause the intensity of Eu^{3+} increase with temperature, while the later tends to cause the intensity decrease. The temperature-quenching rates in various glasses were obtained. They increase with the increasing concentration of Nb_2O_5. The temperature dependencies of the peak locations and the line widths of $^5D_0 - {}^7F_J (J=0,1)$ were experimentally determined.

ACKNOWLEDGMENTS

[1] M. Nogami and Y. Abe, J. Non-Cryst. Solids **197**, 73 (1996).
[2] R. Reisfeld and C. J. Jorgensen, *Handbook on the Physics and Chemistry of Rare Earths* (North-Hollands, Amsterdan, 1987).
[3] M. Nogami, N. Umchara, and T. Hayakawa, Phys. Rev. B **58**, 6166 (1998).
[4] M. Nogami and Y. Abe, J. Opt. Soc. Am. B **15**, 680 (1998).
[5] M. Nogami, T. Nagakura, I. Hayakawa, and T. Sakai, Chem. Mater. **10**, 3991 (1998).
[6] H. Toratani, T. Izumitani, and H. Kuroda, J. Non-Cryst. Solids **52**, 303 (1982).
[7] J. R. Morgan, E. P. Chock, W. D. Hopewell, M. A. Elsayd, and R. Orbach, J. Phys. Chem. **85**, 747 (1981).
[8] S. Tanabe, S. Todoroki, K. Hirao, and N. Soga, J. Non-Cryst. Solids **122**, 59 (1990).
[9] K. Hirao and N. Soga, J. Am. Ceram. Soc. **68**, 515 (1985).
[10] T. F. Belliveau and D. J. Simkin, J. Non-Cryst. Solids **110**, 127 (1987).
[11] M. Nogami, T. Yamazaki, and Y. Abe, J. Lumin. **78**, 63 (1998).
[12] B. R. Judd, Phys. Rev. **127**, 750 (1962).
[13] G. S. Ofelt, J. Chem. Phys. **37**, 511 (1962).
[14] S. Huang, T. Laishui, and L. Lou, Phys. Rev. B **24**, 59 (1981).
[15] G. S. Ofelt, J. Chem. Phys. **38**, 2171 (1963).
[16] P. Porcher and P. Caro, J. Chem. Phys. **68**, 4176 (1978).
[17] V. G. Plotnichenko, V. O. Sokolov, E. B. Kryukova, and E. M. Dianov, J. Non-Cryst. Solids **270**, 20 (2000).
[18] O. Peitl, E. D. Zanotto, and L. L. Hench, J. Non-Cryst. Solids **292**, 115 (2001).
[19] S. A. MacDonald, C. R. Schardt, D. J. Masiello, and J. H. Simmons, J. Non-Cryst. Solids **275**, 72 (2000).
[20] P. Pernice, A. Aronne, V. Sigaev, and Kupriyanova, J. Non-Cryst. Solids **275**, 216 (2000).
[21] B. Tischendorf, J. U. Otaigbe, J. W. Wiench, M. Prusaki, and B. C. Sales, J. Non-Cryst. Solids **282**, 147 (2001).
[22] J. Wang, H. Song, H. Xia, X. Kong, and W. Xu, J. Appl. Phys. **91**, 9466 (2002).